ELSEVIER

Journal of Molecular Catalysis A: Chemical 177 (2002) 289–298

JOURNAL OF MOLECULAR CATALYSIS A: CHEMICAL

www.elsevier.com/locate/molcata

Periodic density functional study of superacidity of sulfated zirconia

Tomonori Kanougi*, Takashi Atoguchi, Shigeru Yao

Polymer Laboratory, Ube Industries, Ltd., Goi-minamikaigan 8-1, Ichihara 290-0045, Japan

Received 14 March 2001; received in revised form 30 May 2001; accepted 26 June 2001

Abstract

Periodic density functional theory (DFT) study was performed in order to investigate structural properties as well as electronic states of the sulfated zirconia (S-ZrO_2) surface. It was found that H_2SO_4 dissociatively adsorbs on the tetragonal (1 0 1) ZrO_2 (t-ZrO_2) surface affording H_2O and SO_3 molecules. The NH_3 adsorption analysis was also performed in order to evaluate the acid strength of both Brönsted and Lewis acid sites on the ZrO_2 surface. In the case of Brönsted acid sites, the proton on H_2O and SO_3 co-adsorbed t-ZrO_2 surface shows stronger acidity than that of H_2O solely adsorbed t-ZrO_2 surface. On the H_2O and SO_3 co-adsorbed tetragonal surface, electron transfer from H_2O molecule into ZrO_2 surface accompanied by that from ZrO_2 surface into SO_3 molecule, was observed. The analysis of Lewis acidity indicated that coordinatively unsaturated surface Zr atom which interacted with SO_3 molecule showed strong Lewis acidity.

Keywords: Periodic density functional theory; Superacidity; Sulfated zirconia

1. Introduction

Sulfate-modified zirconia (S-ZrO_2), which has superacidic surface, shows a superior acid catalytic activity for many reactions such as isomerization of hydrocarbons [1]. After the discovery of the acidic catalytic activity of S-ZrO_2, a lot of studies have been performed from various points of view in order to improve the catalytic activity for the last 20 years [2–9]. The catalytic activity of S-ZrO_2 strongly depends on the preparation method and the calcination temperature. Therefore, various characterizations of the surface and bulk structure of S-ZrO_2 have been carried out in order to elucidate the active structure of the catalyst.

Concerning to the crystal phase of S-ZrO_2, some workers claim a necessity of a tetragonal phase for the catalytic activity for reactions that need strong acid sites. For instance, Morterra et al. [10] prepared several sulfate-doped ZrO_2 catalysts of different crystal phases. From their results, it is concluded that the sulfated tetragonal phase ZrO_2 is catalytically active for the isomerization of *n*-butane, no matter what the preparation route has been, whereas the sulfated monoclinic phase ZrO_2 indicates very low activity for the reaction. However, it has not been clarified well why the tetragonal phase is effective for catalytic reactions such as hydrocarbon isomerization.

The surface structure of S-ZrO_2 has been also studied enthusiastically in order to understand the nature of the active sites. Part of the suggested schemes of S-ZrO_2 surface is summarized in Table 1. Almost of all workers commonly predict SO_x or HSO_x species

* Corresponding author. Tel.: +81-436-22-1391; fax: +81-436-22-3348.
E-mail address: 31132u@ube-ind.co.jp (T. Kanougi).

1381-1169/02/$ – see front matter
PII: S1381-1169(01)00276-X

Table 1
S-ZrO_2 surface models proposed by various workers

Authors	Technique	S-ZrO_2 surface model	Reference
T. Yamaguchi	IR	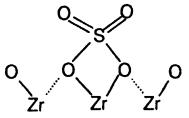	[11]
M. Bensitel et al.	FTIR	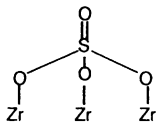	[12]
K. Arata and M. Hino	IR of adsorbed pyridine XPS	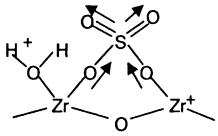	[13]
T. Riemer et al.	^{1}H MAS NMR Raman	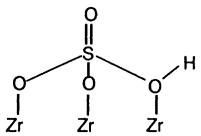	[14]
A. Clearfield et al.	IR ^{1}H MAS NMR TGA	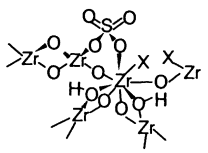	[15]]
L.M. Kustov et al.	IR	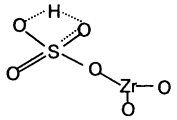	[16]
F. Babou et al.	IR	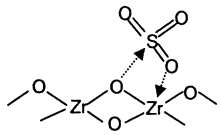	[17]
V. Adeeva et al.	FTIR ^{1}H MAS NMR Temperature-programmed desorption (TPD), Temperature-programmed oxidation (TPO)	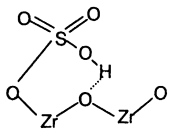	[18]
R.L. White et al.	IR TG–MS	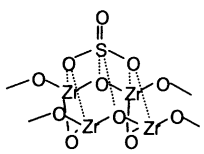	[19]

combined with ZrO_2 surface as S-ZrO_2 surface structure. However, different SO_x or HSO_x species are suggested by them based on their experimental observations. For example, using IR measurement, Yamaguchi [11] has proposed a scheme for the surface sulfated species, where two S=O bonds exist in SO_4^{2-} species. In contrast, only one S=O bond is detected by FTIR measurement done by Bensitel et al. [12]. Other than their works, various workers [13–19] have speculated various superacidic surface structures of S-ZrO_2. Nevertheless, no distinct structure of the superacid sites has been clarified so far and the subject is still under discussion.

On the other hand, recent progress of computer hardware and software allows us to apply computational chemistry to investigate structural and electronic properties of solid catalysts [20–24]. In a situation in which experimental techniques cannot be applied well due to the complexity of the objects, it happens frequently that the computational techniques can be very helpful. For the calculation of surface properties of solid catalysts, both cluster model method and periodic model method are commonly employed. In the cluster model method, a small cluster of a catalytic active site is cut out and reactivity or surface properties are discussed on the cluster model. Babou et al. applied this technique in order to study S-ZrO_2 [25]. They modeled (0 0 1) face of ZrO_2 using $Zr(OH)_4$ tetrahedron and two additional water molecules which interact with Zr atom, and they concluded that a sulfuric acid strongly H-bonded to two oxygen atoms of ZrO_2 surface. Hong et al. also studied initiation processes for butane isomerization over a small sulfated ZrO_2 cluster model [26] and discussed from both experimental and theoretical point of view. Periodic model method was first applied for S-ZrO_2 by Hasse and Sauer [27]. They studied the interaction of a sulfuric acid with (1 0 1) and (0 0 1) surfaces of tetragonal phase ZrO_2. Furthermore, they tried to evaluate the surface Brönsted acidity of S-ZrO_2 by calculating deprotonation energies, however, they could not explain the unique strong acidity of S-ZrO_2 very well.

In the present study, we employed the periodic density functional method and tried to clarify unknown subjects about S-ZrO_2. First of all, adsorption of SO_3 molecule over monoclinic, tetragonal and cubic phase of ZrO_2 surfaces were investigated, aiming to solve the reason why tetragonal phase is effective for some acid reactions. Next, several adsorption states of a sulfuric acid on the tetragonal (1 0 1) surface were assumed and relative stability of the optimized structures was compared. Finally we tried to evaluate the surface acidity of S-ZrO_2 by calculating adsorption energy of NH_3 molecule on our modeled Brönsted and Lewis acid sites.

2. Method and model

Periodic DFT calculations are performed by solving Kohn–Sham equation self-consistently [28] as implemented in DMOL3 software [29–31] on a silicon graphics workstation. The one-electron Schrödinger equations were solved only at the $k = 0$ wavevector point of the Brillouin-zone. The crystal electrostatics of the nuclei and the continuous electronic charge distribution was computed by a modified Ewald method as described in detail in [32]. In order to reduce a computational cost, all core electrons are represented by effective core pseudopotentials (ECP) [29]. Basis sets are represented by the numerical type atomic orbitals, and in this study double numerical with polarization (DNP) basis sets are employed. Vosko–Wilk–Nusair (VWN) local correlation functional [33] is used in order to optimize geometries. More accurate generalized gradient approximation (GGA) in terms of Becke–Lee–Yang–Parr (BLYP) functional [34,35] is also used and the results are compared with those obtained by VWN. For the geometry optimization, BFGS algorithm [29] was employed. The self consistent field (SCF) convergence criteria was set to 10^{-5} ha, and the gradient convergence criteria was set to 10^{-3} ha/Bohr.

Prior to the surface calculations, perfect bulk structures of monoclinic phase ZrO_2 (m-ZrO_2), tetragonal phase ZrO_2 (t-ZrO_2) and cubic phase ZrO_2 (c-ZrO_2) were calculated. Lattice parameters of m-ZrO_2 [36], t-ZrO_2 [37] and c-ZrO_2 [38] were fixed to $a = 5.15$, $b = 5.21$, $c = 5.31$, $\alpha = \gamma = 90.00$, $\beta = 99.23$; $a = b = 7.28$, $c = 10.54$, $\alpha = \beta = \gamma = 90.00$; $a = b = c = 5.08$, $\alpha = \beta = \gamma = 90.00$, respectively. These values were determined on the basis of the experimentally obtained data in [36–38]. Internal atomic positions were fully optimized during calculations. In catalytic reactions, it is very difficult to know which mirror plane of the catalyst is involved

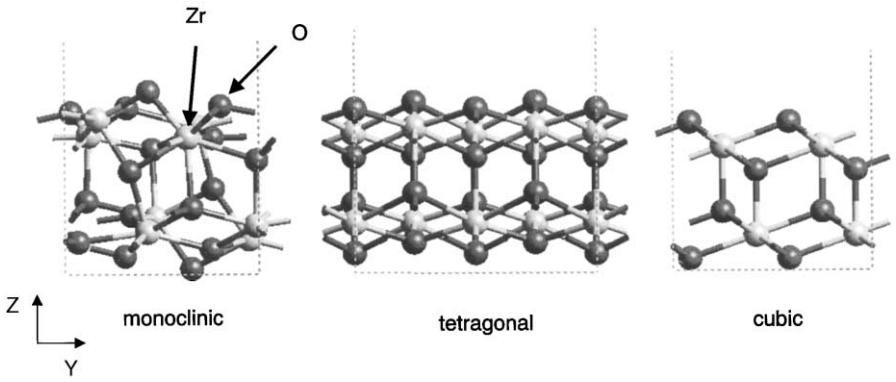

Fig. 1. The CG images of the ZrO_2 surface models (two-layer thickness).

with the actual reaction. However, we have to specify the surface during a modeling procedure in a theoretical study. Therefore, we selected (−1 1 1), (1 0 1) and (1 1 1) surfaces for m-ZrO_2, t-ZrO_2 and c-ZrO_2, respectively, in accordance with surface energy calculation results [27,39,40]. Our surface investigation was performed using a slab–gap model [41]. In this method, the optimized bulk structure is cut along with the specified plane and a new unit cell is created which has the specified plane as the surface of the new cell. In the next step, empty space that has adequate height is created along with z-axis and only 2D periodicity is taken into account. Our modeled slabs have two- and four-layer thickness and each layer is comprised 4 Zr and 8 O atoms. In our calculations, atomic positions of the bottom layer were fixed to those in the bulk structure and upper layer and adsorbates were fully optimized. The CG images of ZrO_2 surface models (two-layer thickness) are shown in Fig. 1. When a sulfuric acid is put on our modeled ZrO_2 surface, coverage by sulfate on m-ZrO_2, t-ZrO_2 and c-ZrO_2 are ca. 2.3, 2.1 and 2.2 atoms nm^{-2}, respectively. These values are very close to 2.5 atoms nm^{-2} of the experimentally measured value [42].

3. Result and discussion

3.1. Coordination number analysis of clean surfaces

Surface structures of m-ZrO_2 (−1 1 1), t-ZrO_2 (1 0 1) and c-ZrO_2 (1 1 1) are relaxed and their coordination environments are compared. In a unit cell of our surface models, four Zr atoms and eight O atoms constitute one ZrO_2 layer, and four Zr atoms and four O atoms among their atoms are exposed to an empty space over the surface. In the bulk structure of m-ZrO_2, Zr atoms are coordinated to seven O atoms and O atoms are coordinated to four Zr atoms. After m-ZrO_2 bulk structure is cleft along with (−1 1 1) plane, coordination number of three surface Zr atoms changes from 7 to 6 while that of one Zr atom remains 7. For O atoms, three surface O atoms change their coordination number from 4 to 3 while one surface O atom changes from 4 to 2. Situation is not so complicated in the case of t-ZrO_2 and c-ZrO_2. In both cases, Zr and O atoms in an original bulk structure are eight- and four-fold coordinated, respectively. However, after the cleavage of the bulk structure, surface Zr and O atoms changes to seven- and three-fold coordinated, respectively. No reconstruction is observed for all surfaces after the relaxation.

3.2. Adsorption of SO_3

Interestingly, it has been shown that S-ZrO_2 which is active for 1-butane isomerization can be prepared by heating a zirconium oxide (ZrO_2) in the presence of SO_3 whereas a similar thermal treatment in the presence of SO_2 without added O_2 does not result in the catalytic activity [43]. While, by using TG–MS technique, it has been found that the primary products of S-ZrO_2 after thermal decomposition are SO_2 and O_2, and that SO_2:O_2 ratio is 2:1 [19]. This

result suggests that the thermal decomposition results in a stoichiometric loss of SO_3 from S-ZrO_2 samples (White's model in Table 1). From the above works, we can guess that SO_3 adsorption on the ZrO_2 surface plays an important role for determining the structure of acid site.

In the present work, we employ two-layer thickness slab model in order to reduce a computational cost. However, it is important to check how slab thickness affects the calculated results. Therefore, in the first step, we have investigated SO_3 adsorption both on two- and four-layer slab models of c-ZrO_2 (1 1 1) surface. In the case of four-layer slab model, bottom one layer is fixed and upper three layers and SO_3 molecule are fully relaxed. Geometries of adsorbed SO_3 molecule, Mulliken charges of constituting atoms and adsorption energies of SO_3 molecule are compared. Here, the adsorption energy is calculated from a following equation:

$$E_{ads} = E_{complex} - (E_{adsorbate} + E_{slab})$$

where E_{ads} is adsorption energy, $E_{complex}$ the energy of a slab model with an adsorbate, and $E_{adsorbate}$ and E_{slab} are energies of an isolated adsorbate and a ZrO_2 slab, respectively. Results are shown in Table 2 (Fig. 2c for the geometry of adsorbed SO_3 molecule on two-layer thickness ZrO_2 surface). Surprisingly, structures of adsorbed SO_3 on these two surfaces are almost same, although a little difference of O_{Zr}-Zr distances is found between two- and four-layer thickness ZrO_2. Therefore, it is probable that layer thickness does not affect the geometry of the adsorbate so much in this system. Mulliken charges of SO_3 molecule on both surfaces are not different so much, although there is a little difference with respect to S atoms that interacts directly with surface O atoms. On the other hand, adsorption energies are largely different between these two systems. Adsorption energy on two-layer slab model tends to be underestimated compared with thicker slab model in regardless of used functionals. In the case of four-layer slab model, upper three layers can be perturbed by the adsorption of SO_3 molecule, while in the case of two-layer slab model, only one layer is allowed to change its atomic positions. This would be the reason why the adsorption energy on two-layer slab model is underestimated.

Next, SO_3 adsorptions on the surfaces of m-ZrO_2, t-ZrO_2 and c-ZrO_2 have been investigated using two-layer slab models. As the initial configuration of the calculation, SO_3 molecule is put parallel to the ZrO_2 surface. Calculated adsorption states of SO_3 molecule on each surface are depicted in Fig. 2. In the case of m-ZrO_2 and c-ZrO_2, SO_3 molecule approaches to the ZrO_2 surface during the calculation, which finally forms one S–O (from ZrO_2) bond and three O–Zr (from SO_3) bonds between SO_3 and the ZrO_2 surface (structures 2a and 2c). On the other hand, SO_3 adsorption on t-ZrO_2 surface gives completely different structure. SO_3 molecule abstracts O atom from t-ZrO_2 surface affording SO_4^{2-} species (structure 2b). From Mulliken population analysis of adsorbed SO_3 species, it is observed that, more electrons transfer from t-ZrO_2 surface into SO_3 molecule compared with the other two surfaces. SO_3 adsorption energy (E_{SO_3}) on each ZrO_2 surface is also calculated. The E_{SO_3} on m-ZrO_2, t-ZrO_2 and c-ZrO_2 surfaces are −57.0, −94.9 and −66.5 kcal/mol, respectively, when VWN is used for correlation functional, and

Table 2
Comparison between two- and four-layer thickness slab models about geometries of adsorbed SO_3 molecule, Mulliken charges of constituting atoms and SO_3 adsorption energies[a]

Layer thickness	Bond length (Å)			Mulliken charges		E_{SO_3} (kcal/mol)	
	S–O_S	S–O_{Zr}	O_{Zr}–Zr	S	O	VWN	BLYP
Two-layer	1.467	1.608	2.250	0.937	−0.378	−57.0	−6.7
	1.469		2.239		−0.373		
	1.471		2.239		−0.371		
Four-layer	1.467	1.609	2.268	0.972	−0.373	−65.8	−12.5
	1.468		2.259		−0.371		
	1.469		2.254		−0.370		

[a] O_S and O_{Zr} represent for oxygen atom from SO_3 molecule and that from ZrO_2 surface, respectively. The structure of the considered ZrO_2 model (two-layer) is shown in Fig. 2(c).

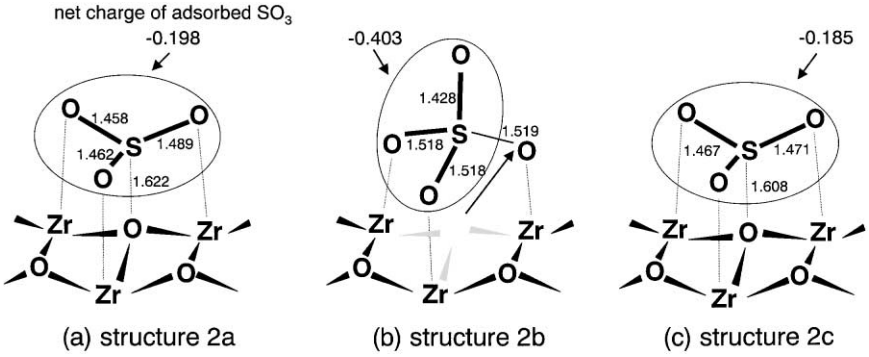

Fig. 2. Adsorption states of SO_3 molecule on (a) m-ZrO_2; (b) t-ZrO_2; and (c) c-ZrO_2 surfaces (bond lengths are represented in angstrom).

−6.7, −52.7 and −17.1 kcal/mol, respectively, when BLYP is used. It has been found that E_{SO_3} with the tetragonal surface is significantly larger than that with the other two surfaces.

It would be wondered that the geometry like 2b is formed also on the surfaces of m-ZrO_2 and c-ZrO_2, if such structure is set as the initial configuration of the calculation. In order to answer such a question, SO_3 adsorption on the surfaces of both m-ZrO_2 and c-ZrO_2 have been studied assuming the initial configurations like structure 2b. For c-ZrO_2, the 2b-like geometry is obtained after the calculation as more stable configuration than the structure 2c; E_{SO_3} at VWN level and BLYP level are −63.6 and −20.5 kcal/mol, respectively. Therefore, from the 2c-like geometry, SO_3 configuration would convert into the 2b-like geometry by going over some energy barrier. For m-ZrO_2, the 2b-like geometry automatically converts to the structure 2a during the calculation. Probably this is due to a less coordination number of surface atoms of m-ZrO_2 than those of t-ZrO_2 and c-ZrO_2. An abstraction of O atom would extremely unstabilize the m-ZrO_2 surface. If superacidity of S-ZrO_2 is related to the geometry represented in structure 2b, the restricted activity of the tetragonal phase will be explained, since the 2b-like geometry is easily formed only on the tetragonal surface.

3.3. Adsorption of H_2SO_4

In this section, several structures of a sulfuric acid on the tetragonal (1 0 1) surface are assumed and relative stability of the optimized structures is discussed. Such calculations have also been done by Haase and Sauer [27], therefore, first we have followed their work about the tetragonal (1 0 1) surface in our calculational condition. According to their work, two configurations of a sulfuric acid on t-ZrO_2 surface represented in Figs. 3 and 4 have been investigated, and consequently we could achieve similar conclusion about these two calculations. In Fig. 3, hydrogen sulfate ion forms three Zr–O bonds with the surface Zr atoms and only one S=O double bond exists in the optimized structure. Here, calculated adsorption energy of a sulfuric acid is −53.4 and −18.5 kcal/mol at VWN and BLYP levels, respectively. Relatively, the value at VWN level

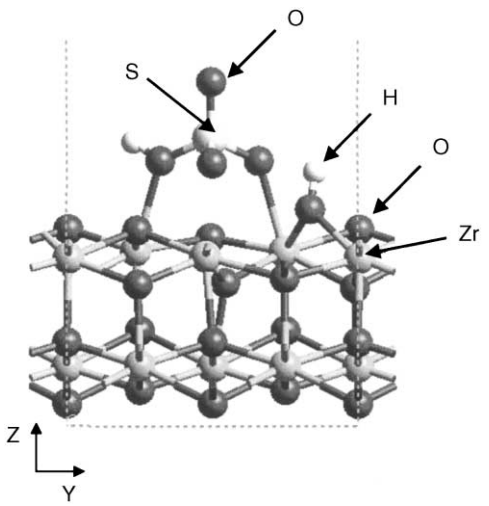

Fig. 3. Configuration of sulfuric acid on the t-ZrO_2 surface (H^+, HSO_4^-).

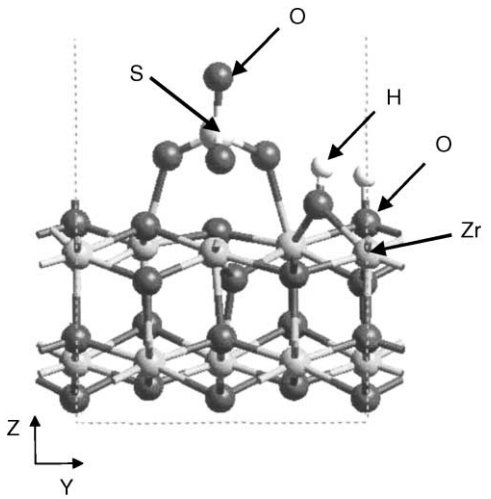

Fig. 4. Configuration of sulfuric acid on the t-ZrO_2 surface ($2H^+$, SO_4^{2-}).

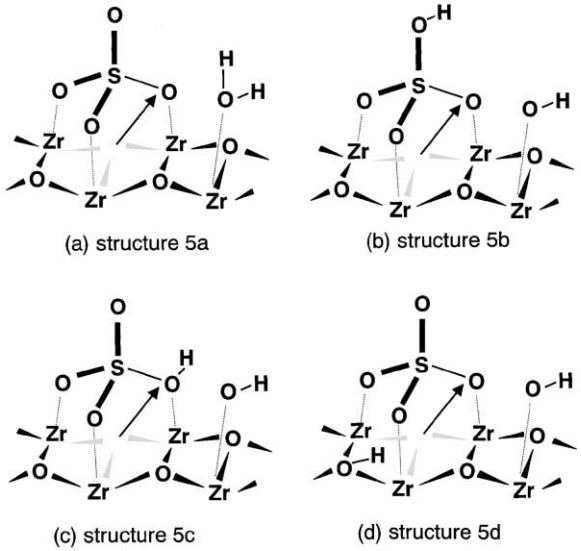

Fig. 5. Schematic configurations of sulfuric acid on the t-ZrO_2 surface.

is close to −56.0 kcal/mol that is estimated at Perdew, Burke and Ernzerhof (PBE) level [44] by Hasse and Sauer [27]. In Fig. 4, a sulfuric acid is completely dissociated into a sulfate anion and two protons. The obtained sulfate anion makes three Zr–O bonds with the surface Zr atoms and two protons form two hydroxyl groups with surface O atoms. Calculated adsorption energy of a sulfuric acid is −74.2 and −25.8 kcal/mol at VWN and BLYP levels, respectively, and as expected, the value at VWN level is close to the Hasse's value of −76.8 kcal/mol.

In addition to the above configurations, we considered other possibilities of H_2SO_4 adsorbed surface structures. Fortunately, we have already found that SO_3 molecule adsorbs on the tetragonal surface at significantly strong affinity. Therefore, based on SO_3 adsorbed surface, we assumed four models of H_2SO_4 adsorbed surfaces as represented in Fig. 5. Interaction energies of an isolated sulfuric acid with the tetragonal surface ($E_{H_2SO_4}$) are given in Table 3. In the structure 5c, an H atom connected to SO_3 species moves to the direction of a surface hydroxyl group and forms H_2O species during the relaxation procedure. Consequently, the structure 5c changes to the geometry like structure 5a. The results in Table 3 indicate that the structure 5a is extremely stable even though compared with the structures shown in Figs. 3 and 4. Therefore, we can say that the structure 5a is the most probable structure of the acid sites of the S-ZrO_2 surface which is not clarified so far. Geometric and electronic properties of the structure 5a are shown in Fig. 6. Two O–H bond lengths of 0.980 and 0.985 Å are almost equal to those of water molecule, therefore, the structure 5a is considered to be a surface where H_2O and SO_3 molecule are co-adsorbed side by side.

Mulliken atomic charges of this system are also investigated. Negative net charge on SO_3 molecule (−0.464) indicates that electron transfer occurs from the ZrO_2 surface into SO_3 molecule. While, positive net charge on H_2O molecule (0.220) indicates that electron transfer occurs from neighboring H_2O molecule into the ZrO_2 surface. With respect to this geometry, vibrational frequency of SO_3

Table 3
Interaction energies of the isolated sulfuric acid with the t-ZrO_2 surface

Models	$E_{H_2SO_4}$	
	VWN (kcal/mol)	BLYP (kcal/mol)
Structure 5a	−96.1	−59.2
Structure 5b	−60.2	−24.1
Structure 5c	Change to structure 5a	
Structure 5d	−57.1	−4.6

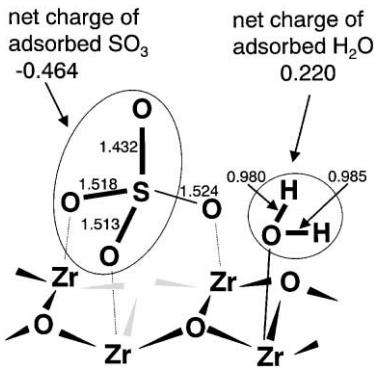

Fig. 6. Configuration of sulfuric acid on the t-ZrO_2 surface (H_2O, SO_3), (bond lengths are represented in angstrom).

species have been calculated by diagonalizing the Cartesian–Hessian matrix constructed by numerical differentiation of the analytical gradients. A scaling factor of 1.02, which is obtained by adjusting the calculated normal modes of SO_3 molecule to the experimental results, is used in order to cancel the DFT results error. In this calculation, totally 4 normal modes have been obtained concerning about SO_3 species. They are assigned to S=O stretch frequency of 1378 cm^{-1} and three S–O stretch frequencies of 1039, 1018 and 1000 cm^{-1}, respectively. These values are good agreement with the corresponding frequencies obtained by infrared measurements [14], that are S=O stretch frequency of 1393 cm^{-1} and 1084, 1026 and 987 cm^{-1}, respectively, concerning about S–O stretching.

3.4. Evaluation of the acid strength

Interesting phenomena have been reported by Arata and Hino [13]. They point out from experiments of infrared spectra of adsorbed pyridine, that a conversion of Lewis acid sites to Brönsted acid sites occurs easily by adsorption of water molecules (Arata's model in Table 1). Therefore, if Zr atom of SO_3 adsorbed tetragonal surface (structure 2b in Fig. 2) and H atom of H_2O and SO_3 co-adsorbed tetragonal surface (structure 5a in Fig. 5) are considered to be Lewis and Brönsted acid sites, respectively, our models are consistent with their result. In order to answer such a question, we tried to evaluate the acid strengths of our models. In order to evaluate acid strength of a solid catalyst, NH_3 gas is often utilized as the probe molecule. Since stronger interaction of NH_3 molecule is observed with stronger acid site of the catalyst. Also in this study, acid strength of the calculated model was examined by calculating adsorption energy of NH_3 molecule on Brönsted or Lewis acid site over the model.

First, NH_3 adsorption energy on S-ZrO_2 surface modeled in this study (Fig. 6) has been estimated, considering protons of adsorbed water as Brönsted acid sites. During the calculation, a nitrogen atom of NH_3 molecule makes a bond with a proton, forming NH_4^+ species. In this structure, NH_3 adsorption energy is estimated to be about −32.2 and −13.2 kcal/mol at VWN and BLYP levels, respectively. In order to evaluate the obtained value relatively, NH_3 adsorption energy on H_2O adsorbed tetragonal surface without SO_3 has been also calculated in the same way. Scheme is shown in Fig. 7. The obtained values of −24.4 kcal/mol at VWN level and −6.5 kcal/mol at BLYP level are less than those on H_2O and SO_3 co-adsorbed tetragonal surface at corresponding levels. This result suggests the stronger Brönsted acidity of the adsorbed H_2O with the adjacent SO_3 compared with that of the solely adsorbed H_2O. The reason of the difference can be explained by Mulliken population analysis of adsorbed H_2O molecules. Net change of the solely adsorbed H_2O molecule is 0.044, which suggests that little electron transfer occur between H_2O molecule and the ZrO_2 surface. While, net change of the adsorbed H_2O neighboring on adsorbed SO_3 indicates larger value of 0.220. This result suggests that more electron transfer occur from H_2O molecule into the ZrO_2 surface, which result from the electron transfer from the ZrO_2 surface into SO_3 molecule. Hence, the adsorbed H_2O neighboring

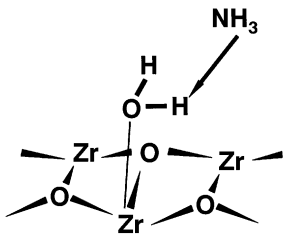

Fig. 7. Scheme of NH_3 adsorption on the H_2O solely adsorbed on ZrO_2 surface.

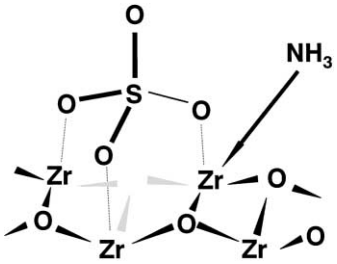

Fig. 8. Scheme of NH_3 adsorption on Lewis acid site on S-ZrO_2 surface.

on SO_3 becomes cationic and shows relatively strong Brönsted acidity.

If Brönsted acid sites is generated by adsorption of water molecule onto Lewis acid site as claimed by Arata and Hino [13], our model shown as the structure 2b is the most probable structure of Lewis acid site. Therefore, we have performed Lewis acid strength analysis in the same way as Brönsted acidity. We assumed a Zr atom bonding to SO_3 molecule as a Lewis acid site, and NH_3 adsorption energy on this site was calculated. Scheme of the model is shown in Fig. 8. The adsorption energies at VWN and BLYP levels are estimated to be −29.7 and −2.1 kcal/mol, respectively. However, obtained values would not be large enough to prove a nature of Lewis acid site on this model, especially at BLYP level. Therefore, another model represented in Fig. 9 was suggested to be a Lewis acid site. In this model, a Zr atom and two O atoms on the surface are deleted in order to create a surface defect. On this acid site, large NH_3 adsorption energies of −56.8 kcal/mol at VWN level and −22.2 kcal/mol at BLYP level are obtained, because of increased Lewis acidity of coodinatively unsaturated Zr atom. This result suggests that a rough S-ZrO_2 surface afford a strong Lewis acid site.

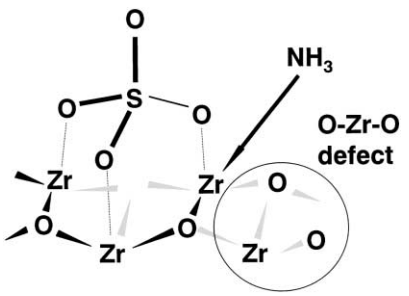

Fig. 9. Scheme of NH_3 adsorption on Lewis acid site on S-ZrO_2 surface which has O–Zr–O defect.

Table 4
NH_3 adsorption energies over several acid sites[a]

Acid site	VWN (kcal/mol)	BLYP (kcal/mol)
H^+ on H_2O/ZrO_2	−24.4	−6.5
H^+ on H_2O, SO_3/ZrO_2	−32.2	−13.2
Zr^+ on SO_3/ZrO_2	−29.7	−2.1
Zr^+ on SO_3/ZrO_2(d)	−56.8	−22.2

[a] SO_3/ZrO_2(d) represents for the SO_3 adsorbed ZrO_2 surface which has the O–Zr–O defect.

NH_3 adsorption energies on several acid sites are summarized in Table 4. For Brönsted acid site, relatively large adsorption energy of NH_3 on H_2O, SO_3/ZrO_2 system is obtained. While, larger adsorption energy of NH_3 on SO_3/ZrO_2(d) system is estimated, although that on SO_3/ZrO_2 system is not so large. It is very difficult to define from the obtained values in the present work whether our modeled surfaces are actually superacidic or not. Using the NH_3 temperature programmed desorption (TPD) technique [42], NH_3 adsorption heats on Brönsted and Lewis acid sites are estimated to be about 36 and 47 kcal/mol, respectively. These values are close to the estimated values at VWN level in this work, although VWN tends to overestimate adsorption energies. However, it is not strange, because our obtained values tend to be underestimated due to the layer thickness effect as explained in Section 3.2.

4. Conclusion

Periodic density functional calculation was performed in order to clarify the nature of the superacidity of the S-ZrO_2 surface. First, SO_3 adsorption on the m-ZrO_2, t-ZrO_2 and c-ZrO_2 surfaces was investigated, and it was found that the affinity of SO_3 with the tetragonal surface was significantly larger than that with other two surfaces. The SO_3 molecule was stabilized affording the SO_4^{2-} species by abstracting the exposed O atom from the ZrO_2 surface. For H_2SO_4 adsorption on the tetragonal surface, several possible configurations were assumed and their energies were compared. The most stable structure was

the H_2O and SO_3, which were produced from H_2SO_4, co-adsorbed tetragonal surface, and then, H_2SO_4 adsorption energy on the surface was estimated to be −96.1 and −59.2 kcal/mol at VWN and BLYP levels, respectively. NH_3 probe method was utilized in order to evaluate the acid strength. From the analysis of Brönsted acidity, it was found that our modeled S-ZrO (SO_3 and H_2O co-adsorbed tetragonal surface) showed relatively strong acidity compared with the H_2O adsorbed tetragonal surface. In the H_2O and SO_3 co-adsorbed tetragonal surface, the electron transfer from H_2O molecule into the ZrO_2 surface accompanied by that from the ZrO_2 surface into SO_3 molecule was observed. Furthermore, the analysis of Lewis acidity indicated that the coordinatively unsaturated Zr atom connected with SO_3 molecule showed strong Lewis acidity, which predicted the higher activity of a rough surface over S-ZrO_2.

References

[1] M. Hino, S. Kobayashi, K. Arata, J. Am. Chem. Soc. 101 (1979) 6439.
[2] C.Y. Hsu, S.R. Heimbuch, C.T. Armes, B.C. Gates, J. Chem. Soc. Chem. Commun. (1992) 1645.
[3] G.D. Karles, J.G. Ekerdt, Prepr. Am. Chem. Soc., Div. Pet. Chem. 37 (1) (1992) 239.
[4] J.R. Sohn, H.W. Kim, J.T. Kim, J. Mol. Catal. 41 (1987) 375.
[5] M. Stoecker, J. Mol. Catal. 29 (3) (1985) 371.
[6] G.D. Yadav, N. Kirthivasan, J. Chem. Soc. Chem. Commun. (1995) 203.
[7] M. Hino, K. Arata, J. Chem. Soc. Chem. Commun. (1995) 789.
[8] G.D. Yadav, J.J. Nair, Langmuir 16 (9) (2000) 4072.
[9] T. Lei, J.S. Xu, Y. Tang, W.M. Hau, Z. Gao, Appl. Catal. A 192 (2000) 181.
[10] C. Morterra, G. Cerrato, F. Pinna, M. Signoretto, J. Catal. 157 (1995) 109.
[11] T. Yamaguchi, Appl. Catal. 61 (1990) 1.
[12] M. Bensitel, O. Saur, J.C. Lavalley, B.A. Morrow, Mater. Chem. Phys. 19 (1988) 147.
[13] K. Arata, M. Hino, Mater. Chem. Phys. 26 (1990) 213.
[14] T. Riemer, D. Spielbauer, M. Hunger, G.A.H. Mekhemer, H. Knozinger, J. Chem. Soc. Chem. Commun.
[15] A. Clearfield, G.P.D. Serrete, A.H. Khazi-Syed, Catal. Today 20 (1994) 295.
[16] L.M. Kustov, V.B. Kazansky, F. Figueras, D. Tichit, J. Catal. 150 (1994) 143.
[17] F. Babou, G. Coudurier, J.C. Vedrine, J. Catal. 152 (1995) 341.
[18] V. Adeeva, J.W. de Haan, J. Janchen, G.D. Lei, V. Schunemann, L.J.M. van de Ven, W.M.H. Sachtler, R.A. van Santen, J. Catal. 151 (1995) 364.
[19] R.L. White, E.C. Sikabwe, M.A. Coelho, D.E. Resasco, J. Catal. 157 (1995) 755.
[20] T. Kanougi, K. Frukawa, M. Yamadaya, Y. Oumi, M. Kubo, A. Stirling, A. Fahmi, A. Miyamoto, Appl. Suf. Sci. 119 (1997) 103.
[21] T. Kanougi, H. Tsuruya, Y. Oumi, A. Chatterjee, A. Fahmi, M. Kubo, A. Miyamoto, Appl. Suf. Sci. 130–132 (1998) 561.
[22] A. Chatterjee, T. Iwasaki, T. Ebina, H. Tsuruya, T. Kanougi, Y. Oumi, M. Kubo, A. Miyamoto, Appl. Suf. Sci. 130–132 (1998) 555.
[23] K. Yajima, Y. Ueda, H. Tsuruya, T. Kanougi, Y. Oumi, S.S.C. Ammal, S. Takami, M. Kubo, A. Miyamoto, Appl. Catal. 194/195 (2000) 183.
[24] M. Yamadaya, H. Himei, T. Kanougi, Y. Oumi, M. Kubo, A. Stirling, R. Vetrivel, E. Broclawik, A. Miyamoto, Stud. Surf. Sci. Catal. 105B (1997) 1485.
[25] F. Babou, B. Bigot, P. Sautet, J. Phys. Chem. 97 (1993) 11501.
[26] Z. Hong, K.B. Fogash, R.M. Watwe, B. Kim, B.I. Masqueda-Jimenez, M.A. Natal-Santiago, J.M. Hill, J.A. Dumesic, J. Catal. 178 (1998) 489.
[27] F. Haase, J. Sauer, J. Am. Chem. Soc. 120 (1998) 13503.
[28] W. Kohn, L.J. Sham, J. Phys. Rev. A 140 (1965) 1133.
[29] DMOL3 version 4.0, San Diego: MSI (1999).
[30] B. Delley, J. Phys. Chem. 92 (1990) 508.
[31] B. Delley, J. Phys. Chem. 94 (1991) 7245.
[32] B. Delley, J. Phys. Chem. 100 (1996) 6107.
[33] S.H. Vosko, L. Wilk, M. Nusair, Can. J. Phys. 58 (1980) 1200.
[34] A.D. Becke, J. Chem. Phys. 96 (1992) 2115.
[35] C. Lee, W. Yang, R.G. Parr, Phys. Rev. B 37 (1988) 786.
[36] D.K. Smith, H.W. Newkirk, Acta Cryst. 18 (1965) 983.
[37] G. Teufer, Acta Cryst. 15 (1962) 1187.
[38] A.P. Bechepeche, O. Teru Jr., E. Longo, J. Mater. Sci. 34 (1999) 2751.
[39] A. Christensen, E.A. Carter, Phys. Rev. B 58 (1998) 8050.
[40] S. Gennard, F. Cora, C.R.A. Catlow, J. Phys. Chem. B 103 (1999) 10158.
[41] C.R.A. Catlow, L. Ackermann, R.G. Bell, F. Cora, D.H. Gay, M.A. Nygren, J.C. Pereira, G. Sastre, B. Slater, P.E. Sinclair, Far. Diss. 106 (1997) 1.
[42] N. Katada, J. Endo, K. Notsu, N. Yasunobu, N. Naito, M. Niwa, J. Phys. Chem. B 104 (2000) 10321.
[43] J.R. Sohn, H.W. Kim, J. Mol. Catal. 52 (1989) 361.
[44] J.P. Perdew, K. Burke, M. Ernzerhof, Phys. Rev. Lett. 77 (1996) 3865.